Transcriptome Sequencing Reveals Sex Differences in Human Meniscal Cell Response to Estrogen Based on Dosing Kinetics

Kelsey E. Knewtson[1], Jesus G. Gonzalez Flores[2], Donna M. Pacicca[3,4], Jennifer L. Robinson[1,2]

1. Chemical and Petroleum Engineering Department, University of Kansas, Lawrence, KS

2. Bioengineering Program, University of Kansas, Lawrence, KS

3. Children's Mercy Hospital, Kansas City, MO

4. University of Missouri-Kansas City, School of Medicine, Kansas City, MO

Corresponding Author

Jennifer L. Robinson, PhD

1530 West 15th Street Room 4132

Lawrence, KS 66045

Tel: (785) 864-0298

jlrobinson@ku.edu

Running Title

Estrogen affects meniscus gene expression

Author Contributions

K.K. analyzed the data and wrote the manuscript. J.G.F. designed and performed the experiment and reviewed the manuscript. D.P. provided critical interpretation of the data and revised the manuscript. J.R. designed the experiment, supervised the study, and wrote the manuscript. All authors have read and approved of the submitted manuscript.

ABSTRACT: Osteoarthritis is a disease marked by progressive and irreversible hyaline cartilage and fibrocartilage breakdown that affects the lives of millions of patients worldwide. Female sex and menopause are both risk factors for knee osteoarthritis, indicating that estrogen could play a role in this disease. In this study, RNA sequencing was used to determine the effects of estrogen treatment on human meniscal cells. Differences in the number and type of differentially expressed genes were seen based on donor sex, estrogen dose, and dosing kinetics. Significantly more differentially expressed genes were seen from male meniscal cells in response to all dosing conditions compared to female cells. Importantly, more genes were differentially expressed in cells treated with continuous dosing of estrogen, which has been shown to stimulate genomic estrogen signaling, as compared to pulsed dosing. Additionally, functional enrichment analysis revealed that many genes of the extracellular matrix, which is important for joint health and injury repair, were differentially expressed. Overall, this initial study lays the groundwork for future avenues to pursue the effect of estrogen delivery on regenerative pathways. This critical analysis will then inform the design and implementation of estrogen replacement therapies to promote meniscal health and reduce the onset of osteoarthritis.

Keywords: estrogen treatment, meniscus tissue, sex differences, RNA sequencing

INTRODUCTION

An estimated 250 million people have knee osteoarthritis (OA) worldwide,[1] with more than 25 million cases in the United States alone.[2] Patients experience progressive and irreversible cartilage breakdown that leads to pain, immobility, and eventual joint failure. Meniscal tears are the most prevalent intra-articular knee injury and pose significant risk in the development of OA.[3] Knee OA

48 is more common and severe in women than in men, especially post-menopause.[4] Also, tears of
49 the meniscal body are more common in women than in men.[5] Further, recent epidemiological
50 studies have found that meniscal injury rates are higher in female high school athletes than in males
51 competing in comparable sports,[6] and that females require repeat meniscal repair surgeries 2.2x
52 more frequently.[7] These data suggest that sex hormone levels, including estrogen, may play a role
53 in meniscal injury and repair.

54 Estrogen is required for joint health and is used as a therapeutic for joint degenerative
55 conditions. Several studies have found a protective effect of estrogen replacement therapy (ERT)
56 against the development and progression of knee OA in post-menopausal women; however, the
57 effects were modest and did not reach significance.[8-10] Treatment with estrogen or selective
58 estrogen receptor modulators has been shown to improve OA symptoms in humans in some
59 studies, but the results are mixed and inconclusive.[11] While clinical data suggests estrogen protects
60 the knee joint and reduces OA, there is a dearth of *in vitro* and preclinical studies investigating the
61 role of estrogen on meniscal health and repair. A better understanding of the effects of estrogen
62 treatment on the knee is needed to develop therapies to improve joint health in different
63 populations.

64 The physiological effects of estrogen vary depending on concentration and dosing kinetics.
65 High and low concentrations of estrogen are known to have opposite effects on inflammation,[12]
66 gene expression,[13] and stem cell proliferation.[14] Specific 17β-estradiol (E2) effects are dose-
67 dependent and differ between tissues.[15] Additionally, several studies have found that the effect of
68 estrogen varies based on dosing kinetics both *in vitro*[16; 17] and *in vivo*.[18] Typically, estrogen exerts
69 its effects on cells by activating the nuclear estrogen receptors alpha and beta, which then regulate
70 transcription of many genes. However, it is known that estrogen can also have quicker, non-

71 genomic effects on cells.[19] There is evidence that controlling dosing kinetics can control the type
72 of response elicited.[16] Conversely, others have found that if total hormone exposure is kept
73 constant, dosing kinetics do not alter the effects of estrogen.[20]

74 The intricacies of the effects of estrogen are significant given the different levels of
75 estrogen seen in patients of different sexes and stages of life and the different doses and delivery
76 routes used for ERT. Serum estradiol levels in healthy, menstruating women range from 40-400
77 pg/mL (150-1,500 pM) depending on the phase of the menstrual cycle,[21] while levels in pregnant
78 women range from 2,000-20,000 pg/mL (7,300-73,000 pM) depending on trimester.[22] Post-
79 menopausal women typically have serum estradiol levels below 15 pg/mL (60 pM).[21] Healthy men
80 under age 55 average serum estradiol levels less than 40 pg/mL (150 pM),[21; 23; 24] and these levels
81 decrease as men age and their testosterone levels decrease.[24] Average serum levels of estradiol
82 achieved by ERT typically range from 20-100 pg/mL.[25] Less data is available on synovial fluid
83 (SF) estradiol levels, which is the most pertinent data for tissues such as the meniscus. The data
84 available for SF is mostly limited to older patient populations with OA or rheumatoid arthritis
85 (RA). These studies have found estradiol SF levels ranging from 15-54 pg/mL (60-200 pM) in
86 male and female patients, with higher levels typically seen in RA patients than in OA patients.[26-
87 28] Though these levels cannot be applied to other populations, these studies did find strong, positive
88 linear correlations between serum and SF estradiol levels that could be applicable to other groups.
89 In terms of ERTs, each treatment type (e.g. formulation and deployment form) is associated with
90 a different hormone exposure level and kinetic profile. For example, though a 50 μg/day
91 transdermal reservoir patch, 2 mg oral tablet, and 300 μg nasal dose of E2 all provide similar 24 h
92 systemic exposures (1080-1400 pg*h/ml), they each have a unique kinetic profile ranging from
93 continuous over days with a transdermal patch to pulsed over hours with a nasal delivery route.[29]

94 Further studies are needed to understand the effects of estrogen concentration and dosing kinetics
95 on tissues of interest from different patient populations.
96 In this study, we aimed to both determine sex differences and the role of concentration and
97 dosing kinetics on human knee meniscal cell gene expression changes in response to estrogen
98 treatment. Cells were isolated from the menisci of two age-matched donors, one of each sex, and
99 treated with two concentrations of 17β-estradiol (E2) under pulsed and continuous conditions.
100 Messenger RNA sequencing (RNA-Seq) was then used to determine differentially expressed genes
101 as a function of the E2 treatment groups. Results from this study will inform future work on
102 developing a mechanistic understanding of estrogen delivery conditions on cell and tissue response
103 to aid in design and development of treatments for knee injury based on patient sex.
104

105 **METHODS**

106 **Cells and Treatment**

107 The experimental design and workflow are illustrated in Figure 1. Human meniscal tissue was
108 received from the National Disease Research Interchange (NDRI). Cells were harvested from the
109 medial meniscus of a human cadaveric male (Black) and a female (Caucasian) (both 47-year old).
110 Briefly, whole menisci were cut into small pieces (1-2 mm) and digested in DMEM (11996-065,
111 Gibco, Carlsbad, CA) containing 2% penicillin/streptomycin (15140-122, Gibco, Carlsbad, CA)
112 and 3 mg/mL collagenase type I (17100-017, Gibco, Carlsbad, CA) at 37 °C and 60 rpm for 16 h.
113 Solutions were filtered through Swinnex Filter Holders (25 mm, SX0002500, Sigma-Aldrich, St.
114 Louis, MO) loaded with Spectra Mesh Nylon Filters (30 μM, 888-13681, Spectrum Chemical
115 Manufacturing Corporation, New Brunswick, NJ) to remove undigested tissue. Cells were then
116 cultured in T75 tissue culture treated flasks in DMEM supplemented with 10% Premium FBS

117 (511150, Atlanta Biologicals, Minneapolis, MN) and 1% penicillin/streptomycin. After reaching
118 confluency, cells were passaged using trypsin (T4174, Sigma, St. Louis, MO, diluted to 1x before
119 use) and seeded into T225 tissue culture treated flasks. When passage 1 cells reached 70-80%
120 confluency, cells were washed with PBS (20012-207, Gibco, Carlsbad, CA) and cultured in phenol
121 red-free DMEM (pfDMEM, 31053-028, Gibco, Carlsbad, CA) with 15% charcoal/dextran treated
122 FBS (S11650, Atlanta Biologicals, Minneapolis, MN) for 3 days to starve them of endogenous
123 hormones. Cells were then passaged and seeded at 10,000 cells/cm^2 in 24 well plates in pfDMEM
124 and allowed to adhere overnight. The next day, cells were treated in triplicate with 17β-estradiol
125 (E2, E2758, Sigma, St. Louis, MO) in pfDMEM supplemented with 15% charcoal/dextran treated
126 FBS and 1% penicillin/streptomycin under pulsed or continuous dosing. For pulsed dosing, cells
127 were exposed to E2 (0, 24, or 240 μM) for 1 h, after which the E2 media was replaced with E2-
128 free media for 23 h. This pattern was repeated for a total of 72 h. For continuous dosing, cells were
129 exposed to E2 (0, 1, or 10 μM) for the entire treatment period of 72 h. The different concentrations
130 used for pulsed compared to continuous dosing were used so that the total 24 h exposure was
131 identical between groups, as reported previously.[16; 17; 20] The concentrations used were chosen to
132 be above normal physiological levels in order to elicit a significant response. Further, 1 μM is
133 predominantly used as a high concentration in *in vitro* estrogen dosing studies. Different dosing
134 kinetics were used to mimic those seen with different types of estrogen replacement therapies such
135 as pulsed from nasal doses of E2 and continuous from transdermal patches.
136

137 **RNA Extraction, cDNA Library Construction, and Sequencing**

138 After 72 h, cells were collected in TRIzol, and total RNA was purified using the manufacturer's
139 protocol. DNA was removed using a DNA-*free* DNA Removal Kit (AM1906, Life Technologies,

140 Grand Island, NY). Total RNA samples were quality checked with a Qubit Assay and Agilent
141 TapeStation for quantity and quality, respectively. All RNA preps had an estimated RIN value that
142 ranged from 8.8-10. Sequencing libraries were constructed using the NEBNext Ultra II
143 Directional RNA Library Prep Kit for Illumina (E7760, New England BioLabs, Ipswich, MA).
144 The library preps were started with 92-1000 ng of total RNA. The sequencing library construction
145 process includes mRNA purification with polyA selection beads, fragmentation to inserts of ~200
146 bp, strand specific cDNA synthesis, end repair, 3' end adenylation, adapter ligation, and PCR
147 amplification. The constructed sequencing libraries were validated and quantified with Qubit and
148 TapeStation assays. Each library was indexed with a barcode sequence and sequenced in a
149 multiplexed fashion. An Illumina NextSeq 550 system at the University of Kansas's Genome
150 Sequencing Core was used to generate single-end, 100-base sequence reads from the libraries.
151

152 **Data Processing**

153 Base calling was carried out by the instrument Real Time Analysis (RTA) software. The base call
154 files (bcl files) were demultiplexed and converted to compressed FASTQ files by bcl2fastq2. Raw
155 reads were filtered using fastp,[30] retaining only reads longer than 40 nucleotides. Processed reads
156 were then pseudoaligned to the human reference transcriptome (ensembl.org, release 97, build
157 GRCh38) using kallisto,[31] employing 100 bootstraps to estimate transcript abundance. tximport[32]
158 was then used to import kallisto transcript abundance estimates into DESeq2[33] for differential
159 expression analysis. Within DESeq2, a series of pairwise likelihood ratio tests to identify genes
160 showing differential gene expression, considering genes to be differentially expressed for a given
161 test if they survived a 5% False Discovery Rate criterion, was conducted. GraphPad Prism 8 was
162 used to generate volcano plots by plotting the $\log_2$FoldChange against the adjusted P value. Venny

163 2.1[34] was used to generate Venn diagrams of the differentially expressed genes with adjusted p
164 values (padj) < 0.05. Venn diagrams were then redrawn using Adobe Illustrator to allow for color
165 control. Significant results were further analyzed using the Search Tool for the Retrieval of
166 Interacting Genes/Proteins (STRING)[35] to detect protein-protein interactions using the confidence
167 view to display connection thickness based upon strength of the supporting data. Functional
168 enrichment analysis was performed within STRING, with databases and categories selected based
169 upon first significance and then ability to highlight gene clusters. The Database for Annotation,
170 Visualization and Integrated Discovery (DAVID)[36] was used for further functional enrichment
171 analysis with the human genome used as the background. The Gene Ontology Cellular Component
172 database was used within the Functional Annotation Chart function of DAVID. Heat maps were
173 generated using GenePattern.[37] To generate the list of extracellular matrix genes, the genes
174 identified within this category by DAVID for each treatment group were compiled into a master
175 list of ECM genes. The $\log_2$FoldChange for these genes were then gathered from each treatment
176 group and used uploaded to the Heat Map Image module of GenePattern. Column and row sizes
177 were set to 128 pixels, the color scheme was globally normalized, and color gradient was not used.
178

179 **RESULTS**

180 **Male Meniscal Cells Respond More Robustly to Estrogen Treatment**

181 The number of genes in each treatment group that were differentially expressed (DEGs) as
182 compared to the sex-matched no E2 control was plotted in terms of E2 concentration relative to
183 physiological concentrations (Figure 2). This revealed that male cells responded more strongly to
184 E2 treatment than female cells. In general, more DEGs were seen from groups treated with
185 continuous dosing than for groups treated with pulsed dosing, though the male high dose pulsed

186 group had the most DEGs of all treatment groups. Additionally, within the female treatment
187 groups, there were greater differences in the number of DEGs based on dosing kinetics than on
188 concentration. In males, E2 concentration had a large effect on DEG count for the pulsed groups,
189 an effect that does not trend with the other comparisons in which concentration did not play as
190 significant a role when controlling for kinetics.

191 Volcano plots were generated to visualize the number of DEGs in each treatment group in
192 terms of fold change and adjusted P value (Figure 3A). These plots show that in most treatment
193 groups, the majority of DEGs had a $\log_2$FoldChange between -2 and 2, though most groups had at
194 least one gene that fell far outside this range. Examples include POLR2J3 in the female high dose
195 pulsed group ($\log_2$FoldChange -7.98) and GNL1 in the male high dose pulsed group
196 ($\log_2$FoldChange 9.94)

197 The Venn diagrams in Figure 3B illustrate more overlap in the DEGs of the male treatment
198 groups compared to the female groups. In fact, 230 genes were common to all 4 groups. Further
199 analysis of these overlapping genes can be seen in Table S1 and Figure S1. This analysis revealed
200 that many groups of genes, including those of the extracellular matrix (ECM), were enriched in
201 this set and that there were many protein-protein interactions among the genes. The highest overlap
202 in DEGs occurred between the male high dose groups, where 823 DEGs were seen in both groups
203 (262 genes that only overlap between the high dose groups and 561 that also overlap with other
204 groups). Comparatively, the highest overlap in female meniscal cell treatment was seen in the
205 continuous treatment groups, where 20 DEGS were seen in both groups.

206

207 **Types of DEGs Differ Based on Estrogen Dosing Concentration and Kinetics and Sex**

208 The DEGs from each continuous dosing treatment group were then analyzed using STRING[35]
209 (Figure 4). Additional constraints based on log_2FoldChange were used to limit DEGs to a
210 reasonable number for visualization and to highlight those with greater fold changes compared to
211 control. STRING analysis of the other treatment groups and images without log_2FoldChange
212 constraints can be found in Figures S2-S4. Functional enrichment analysis was also performed
213 within STRING, as indicated by the color coding of certain proteins. This revealed that the DEGs
214 of both female continuous dosing groups were enriched for proteins of the ECM, which is of
215 interest for its importance to joint healing. In the male continuous groups, low dose resulted in
216 DEGs related to metabolic pathways involving nitrogen and high dose resulted in DEGs involved
217 in gene expression and thyroid hormone signaling pathways.
218
219 **Conservation of DEGS in Continuous Treatment Groups of Both Sexes**
220 Additional analysis was done to compare the effects of the same treatment in different sexes
221 (Figure 5). Venn diagrams (Figure 5a) illustrate that relatively few DEGs were common between
222 the same treatment of different sexes, with the most overlap occurring between the high dose
223 continuous groups. Interestingly, in the continuous dosing groups with low and high dose, four
224 genes are conserved in both female and male cells indicating similar control of estrogen on the
225 transcription of these genes. The proteins for which these genes encode function as facilitators of
226 transport across cell membranes (*SLC7AA1 and ABCC1),* protease that functions to cleave insulin-
227 like growth factor binding proteins necessary for bone formation, inflammation, wound healing,
228 and fertility (*PAPPA1 and 2)*, and transcription factor and ubiquitin binding (*UBXN7)*. The
229 complete list of these overlapping DEGs can be found in Table S2. DAVID analysis (Figure 5b)
230 revealed several groups enriched in these datasets compared to the human genome including

231 extracellular exosomes in the low dose continuous treatments and extracellular space in the high
232 dose continuous groups. STRING[35] analysis (Figure 5c) illustrated that there were few protein-
233 protein interactions between these genes. However, interactions controlling cell cycle processes
234 (PAPPA/PCNA/TMSB4X) and TGFβR1/SMAD9, both important for meniscus cell proliferation
235 and phenotype, were highlighted in the high dose continuous groups of both sexes.

236 Overlapping DEGs as a function of treatment in the female groups are shown in Figure 6.
237 Overall, continuous dosing exhibited the most conserved DEGs with estrogen concentration
238 (Figure 6a). In looking at the pathway enrichment (Figure 6b) and protein-protein interactions
239 (Figure 6c), genes involved in repair and homeostasis of the ECM are reported. All 20 DEGs of
240 this group are shown with their expression in all other groups in the heat map in Figure 6d. The
241 major genes regulated were all protein coding genes that are implicated in cell-cell signaling
242 (*ACKR4, CLDN11),* or cell differentiation (*PAMR1, S100A4, and S100A5*). A full list of these
243 genes can be found in Table S3.
244

245 **DEGS Related to the Extracellular Matrix from Estrogen Treatment**

246 Functional enrichment analysis using DAVID[36] showed that the types of genes enriched varied
247 depending on donor sex, E2 dose, and dosing kinetics (Figure 7). Of interest for joint healing,
248 genes of the ECM, highlighted in red, were enriched in all treatment groups except the female
249 pulsed dosing groups. Genes related to extracellular exosomes and focal adhesion were enriched
250 in all the male treatment groups plus the female low dose continuous group. Membrane, cytoplasm,
251 and cytosol genes were enriched in all male treatment groups but none of the female treatment
252 groups. Genes of the actin cytoskeleton were only enriched in both male low dose groups. Nucleus
253 genes were enriched in all male groups except low dose pulsed. Genes of the basement membrane,

254 extracellular region, extracellular space, collagen trimer, and endoplasmic reticulum lumen were
255 enriched in both female continuous dosing groups but not in any of the male treatment groups.
256 The importance of estrogen in promoting new extracellular matrix for fibrocartilage tissue
257 regeneration and homeostasis has been previously detailed.[38] For this reason, the relative
258 expression of genes within the ECM category from each treatment group are illustrated in a heat
259 map in Figure 8. Separate heat maps for both sexes, doses, and dosing kinetics can be found in
260 Figures S5-S7. The expression levels of many genes were either up- or down-regulated in all
261 treatment groups. For example, ABI3BP, ADAMTS3, CANX, CDON, FBN1 and 2, LOXL2,
262 LTBP2, TIMP2 and 3, and many collagens were down-regulated in all treatment groups and
263 CALR, CFL1, CRIP2, LOXL1, LTBP3 and 4, and TNXB were up-regulated in all groups. Others
264 such as ACTG1, COL14A1, COL7A1, HMCN1, mATN2, OGN, and PFKP were split by donor
265 sex. No clear patterns were present based on low versus high dose, except for the ribosomal
266 proteins in male treatment groups. Of particular interest to cartilage and fibrocartilage, COMP,
267 POSTN, and TGFB1 and 3 were differentially regulated based on sex and estrogen dosing kinetics.
268

269 **Discussion**

270 A number of microarray and sequencing studies have provided important insight on transcriptome
271 differences in the meniscus including avascular meniscus that heals poorly,[39] in meniscus from
272 patients with and without osteoarthritis,[40] the progenitor cell phenotype that may reduce
273 osteoarthritis,[41] and single-cell sequencing to define unique meniscal progenitor populations that
274 are critical to maintain tissue health and reduce degeneration.[42] Building off this body of work,
275 this study focuses on transcriptome differences between male and female tissue that will inform
276 sex differences in natural aging and inform the role of sex hormones in repair and homeostasis.

277 There is evidence that estrogen replacement therapy can reduce OA incidence and
278 symptoms.[8-11] ERT can also prevent and treat osteoporosis and osteoarthritis. Unfortunately, ERT
279 is not without risk and can have negative off-target effects. Oral use of ERT increases the risk of
280 venous thromboembolism in post-menopausal women.[43] Combination use of estrogen plus
281 progestin, and to a lesser extent estrogen alone, is linked with an increased risk of breast cancer in
282 some studies.[44; 45] The results presented here contribute to the pool of evidence supporting the
283 importance of estrogen dose and kinetics for achieving the desired results in different patient
284 populations. Further studies could lead to knowledge about estrogen dose and kinetics that are
285 needed to develop safe and effective treatments for knee injury and mitigate the need for systemic
286 dosing at high concentrations needed to hit therapeutic dose that lead to deadly, off-target effects.
287 While more DEGs were reported in all of the male treatment groups, a hypothesized effect
288 due to the relative naivety of the male cells to high estrogen doses, an important finding is the
289 interplay between concentration and kinetics in both groups. In most cases, there were more DEGs
290 seen in treatment groups with continuous dosing than with pulsed dosing. This corresponds with
291 the findings of Simoncini *et. al.* that continuous E2 dosing of human umbilical vein endothelial
292 cells (HUVECs) leads to heavier E2 signaling through the traditional genomic pathways than
293 pulsed dosing.[16] In contrast, Cavailles *et. al.* found no difference in the effects of pulsed compared
294 to continuous estrogen dosing on the expression levels of 3 estrogen-responsive genes.[20] This
295 inconsistency can possibly be explained by the different scopes of the studies and different
296 concentrations of E2 used. Another study found more DEGs in HUVECs treated with pulsed
297 estrogen than those treated with continuous estrogen,[17] in direct contradiction to the current study.
298 A possible explanation for this is the differential response to estrogen dosing kinetics based on
299 tissue type seen by Otto *et. al.*[18] Interestingly, with continuous dosing, concentration did not play

300 a major role in total DEGs whereas concentration did play a significant role with pulsed dosing.
301 Also, in the female groups, pulsed dosing resulted in lower total DEGs whereas the total DEGs
302 was a function of concentration in the male groups. Overall, it is likely that continuous dosing is
303 required for the robust transcriptional changes necessary for remodeling and homeostasis to
304 maintain meniscal health and reduce OA.

305 Functional enrichment analysis using DAVID and STRING revealed that the types of
306 genes enriched varied by donor sex, E2 dose, and dosing kinetics. Genes related to the extracellular
307 matrix were enriched in all groups except the female pulsed groups. It is also of interest that the
308 DEGs common to both male and female cells are related to the extracellular matrix. There is
309 evidence that increasing ECM production in joint tissues can improve joint function.[38] While all
310 of the differentially expressed collagens and tissue inhibitors of metalloproteinases (TIMPs) are
311 downregulated within all treatment groups, growth factors such as in the TGFβ family are
312 upregulated in all male groups and in the female pulsed groups. This is information that must be
313 pursued in future studies as TGFβ3 is a major growth factor in meniscus remodeling and repair[46-
314 50] and activation of this protein enhances differentiation ability of meniscus progenitors to
315 chondrogenic-like avascular tissue.[41; 51] Additionally, TNXB, LTBP3, and LTBP4, genes that have
316 each been shown to play a role in the activation, availability, and/or signaling of TGFβ[52; 53], are all
317 upregulated in all groups. LTBP2, another gene in the LTBP family, is down-regulated, but it is
318 also the only one in the family that does not bind to latent TGFβ.[53] TNXB is also important for the
319 correct assembly of other matrix molecules and wound healing.[53] TGFβ stimulates collagen
320 production at the transcription level, so it is interesting that TGFβ expression was up-regulated but
321 collagen expression was down-regulated. A possible explanation is found in Fragiadaki *et. al.*'s
322 report that high doses of TGFβ down-regulate expression of COL1A2.[54]

There are limitations to the current study that should be considered. This study was performed using 2D culture methods, which are known to promote a more fibroblast-like phenotype of the meniscal fibrochondrocytes[39; 55] and thus will indicate more of the fibroblast-like cell response to estrogen. Additionally, this study was performed using cells isolated from only 2 donors, both 47-years old. It is likely that these cells had relatively limited remodeling capability due to the age of the donors. Furthermore, the 2 donors were of different races (Black and Caucasian), which could have been a complicating factor, though one study found no difference in meniscal tear rates between members of white and black racial groups.[56] Future studies on 3D cultures using tissue from more donors of different ages and more concentrations of estrogen could be very informative to elucidate more conclusive effects of estrogen on the meniscus and for the development of treatments for knee injury.

Conclusions

Overall, the estrogen dosing kinetics played a more significant role on total DEG compared to estrogen concentration in both sexes. There were only four DEGs conserved across sexes in both low and high concentrations in continuous dosing illustrating that meniscus cell transcriptional response to estrogen signaling is significantly different between male and females. Future work will expand on this initial data set to probe the effect of specific pathways, such as TGF-β3 known to promote meniscus healing, to provide clear insight into the role estrogen plays on meniscus regeneration and homeostasis. Overall, this initial study lays the groundwork for future avenues to pursue the effect of estrogen delivery on regenerative pathways to inform the design and implementation of ERT therapies to promote meniscal health and reduce the onset of osteoarthritis.

346 **Acknowledgments**

347 We acknowledge the use of tissues procured by the National Disease Research Interchange (NDRI)
348 with support from NIH grant U42OD11158. The authors want to thank Brittney Smith and Jennifer
349 Hackett at the KU Genome Sequencing Center (GSC) for completing the sequencing (NIH NIGMS
350 P20GM103638) and Boryana Koseva and Stuart Macdonald of the K-INBRE Bioinformatics Core
351 for providing computational support (NIH P20 GM103418). Further, the authors are appreciative
352 of the insight and analysis feedback from Dr. Emily Farrow, director of laboratory operations at
353 the Genome Center at Children's Mercy Hospital. This work was supported by startup funds from
354 the University of Kansas (JR) and NIH NIGMS P20GM103638 (KK, JGG, and JLR).

355

356 **References**

357 1. O'Neill TW, McCabe PS, McBeth J. 2018. Update on the epidemiology, risk factors
358 and disease outcomes of osteoarthritis. Best Pract Res Clin Rheumatol 32:312-
359 326.

360 2. Zhang Y, Jordan JM. 2010. Epidemiology of osteoarthritis. Clin Geriatr Med
361 26:355-369.

362 3. Englund M, Roos EM, Lohmander LS. 2003. Impact of type of meniscal tear on
363 radiographic and symptomatic knee osteoarthritis: a sixteen-year followup of
364 meniscectomy with matched controls. Arthritis Rheum 48:2178-2187.

365 4. Srikanth VK, Fryer JL, Zhai G, et al. 2005. A meta-analysis of sex differences
366 prevalence, incidence and severity of osteoarthritis. Osteoarthritis Cartilage
367 13:769-781.

368 5. Ding C, Martel-Pelletier J, Pelletier JP, et al. 2007. Meniscal tear as an
369 osteoarthritis risk factor in a largely non-osteoarthritic cohort: a cross-sectional
370 study. J Rheumatol 34:776-784.
371 6. Mitchell J, Graham W, Best TM, et al. 2016. Epidemiology of meniscal injuries in
372 US high school athletes between 2007 and 2013. Knee Surg Sports Traumatol
373 Arthrosc 24:715-722.
374 7. Patel NM, Mundluru SN, Beck NA, et al. 2019. Which Factors Increase the Risk of
375 Reoperation After Meniscal Surgery in Children? Orthop J Sports Med
376 7:2325967119842885.
377 8. Hannan MT, Felson DT, Anderson JJ, et al. 1990. Estrogen use and radiographic
378 osteoarthritis of the knee in women. The Framingham Osteoarthritis Study. Arthritis
379 Rheum 33:525-532.
380 9. Zhang Y, McAlindon TE, Hannan MT, et al. 1998. Estrogen replacement therapy
381 and worsening of radiographic knee osteoarthritis: the Framingham Study. Arthritis
382 Rheum 41:1867-1873.
383 10. Hart DJ, Doyle DV, Spector TD. 1999. Incidence and risk factors for radiographic
384 knee osteoarthritis in middle-aged women: the Chingford Study. Arthritis Rheum
385 42:17-24.
386 11. Xiao YP, Tian FM, Dai MW, et al. 2016. Are estrogen-related drugs new
387 alternatives for the management of osteoarthritis? Arthritis Res Ther 18:151.
388 12. Straub RH. 2007. The complex role of estrogens in inflammation. Endocr Rev
389 28:521-574.

390 13. Koelling S, Miosge N. 2010. Sex differences of chondrogenic progenitor cells in
391 late stages of osteoarthritis. Arthritis Rheum 62:1077-1087.
392 14. Lee WJ, Lee SC, Lee JH, et al. 2016. Differential regulation of senescence and in
393 vitro differentiation by 17beta-estradiol between mesenchymal stem cells derived
394 from male and female mini-pigs. J Vet Sci 17:159-170.
395 15. Fontaine C, Buscato M, Vinel A, et al. 2020. The tissue-specific effects of different
396 17beta-estradiol doses reveal the key sensitizing role of AF1 domain in ERalpha
397 activity. Mol Cell Endocrinol 505:110741.
398 16. Simoncini T, Fornari L, Mannella P, et al. 2005. Differential estrogen signaling in
399 endothelial cells upon pulsed or continuous administration. Maturitas 50:247-258.
400 17. Li J, Wang H, Johnson SM, et al. 2008. Differing transcriptional responses to
401 pulsed or continuous estradiol exposure in human umbilical vein endothelial cells.
402 J Steroid Biochem Mol Biol 111:41-49.
403 18. Otto C, Kantner I, Nubbemeyer R, et al. 2012. Estradiol release kinetics determine
404 tissue response in ovariectomized rats. Endocrinology 153:1725-1733.
405 19. Azuma K, Inoue S. 2012. Genomic and non-genomic actions of estrogen: recent
406 developments. Biomol Concepts 3:365-370.
407 20. Cavailles V, Gompel A, Portois MC, et al. 2002. Comparative activity of pulsed or
408 continuous estradiol exposure on gene expression and proliferation of normal and
409 tumoral human breast cells. J Mol Endocrinol 28:165-175.
410 21. Sluss PM, Hayes FJ, Adams JM, et al. 2008. Mass spectrometric and physiological
411 validation of a sensitive, automated, direct immunoassay for serum estradiol using
412 the Architect. Clin Chim Acta 388:99-105.

413 22. Schock H, Zeleniuch-Jacquotte A, Lundin E, et al. 2016. Hormone concentrations
414 throughout uncomplicated pregnancies: a longitudinal study. BMC Pregnancy
415 Childbirth 16:146.
416 23. Dighe AS, Moy JM, Hayes FJ, et al. 2005. High-resolution reference ranges for
417 estradiol, luteinizing hormone, and follicle-stimulating hormone in men and women
418 using the AxSYM assay system. Clin Biochem 38:175-179.
419 24. Decaroli MC, Rochira V. 2017. Aging and sex hormones in males. Virulence 8:545-
420 570.
421 25. Stanczyk FZ, Clarke NJ. 2014. Measurement of Estradiol—Challenges Ahead.
422 The Journal of Clinical Endocrinology & Metabolism 99:56-58.
423 26. Rovensky J, Radikova Z, Imrich R, et al. 2004. Gonadal and adrenal steroid
424 hormones in plasma and synovial fluid of patients with rheumatoid arthritis. Endocr
425 Regul 38:143-149.
426 27. Rovensky J, Simorova E, Radikova Z, et al. 2006. Comparison of hormone transfer
427 to pleural and synovial exudates. Endocr Regul 40:29-36.
428 28. Richette P, Laborde K, Boutron C, et al. 2007. Correlation between serum and
429 synovial fluid estrogen concentrations: comment on the article by Sowers et al.
430 Arthritis Rheum 56:698; author reply 698-699.
431 29. Devissaguet JP, Brion N, Lhote O, et al. 1999. Pulsed estrogen therapy:
432 pharmacokinetics of intranasal 17-beta-estradiol (S21400) in postmenopausal
433 women and comparison with oral and transdermal formulations. Eur J Drug Metab
434 Pharmacokinet 24:265-271.

435 30. Chen S, Zhou Y, Chen Y, et al. 2018. fastp: an ultra-fast all-in-one FASTQ
436 preprocessor. Bioinformatics 34:i884-i890.
437 31. Bray NL, Pimentel H, Melsted P, et al. 2016. Near-optimal probabilistic RNA-seq
438 quantification. Nat Biotechnol 34:525-527.
439 32. Soneson C, Love MI, Robinson MD. 2015. Differential analyses for RNA-seq:
440 transcript-level estimates improve gene-level inferences. F1000Res 4:1521.
441 33. Love MI, Huber W, Anders S. 2014. Moderated estimation of fold change and
442 dispersion for RNA-seq data with DESeq2. Genome Biol 15:550.
443 34. Oliveros JC. 2007-2015. Venny-An interactive tool for comparing lists with Venn's
444 diagrams.
445 35. Szklarczyk D, Gable AL, Lyon D, et al. 2019. STRING v11: protein-protein
446 association networks with increased coverage, supporting functional discovery in
447 genome-wide experimental datasets. Nucleic Acids Res 47:D607-d613.
448 36. Huang da W, Sherman BT, Lempicki RA. 2009. Systematic and integrative
449 analysis of large gene lists using DAVID bioinformatics resources. Nat Protoc 4:44-
450 57.
451 37. Reich M, Liefeld T, Gould J, et al. 2006. GenePattern 2.0. Nat Genet 38:500-501.
452 38. Robinson JL, Soria P, Xu M, et al. 2018. Estrogen Promotes Mandibular Condylar
453 Fibrocartilage Chondrogenesis and Inhibits Degeneration via Estrogen Receptor
454 Alpha in Female Mice. Sci Rep 8:8527.
455 39. Grogan SP, Duffy SF, Pauli C, et al. 2018. Gene expression profiles of the
456 meniscus avascular phenotype: A guide for meniscus tissue engineering. J Orthop
457 Res 36:1947-1958.

458 40. Brophy RH, Zhang B, Cai L, et al. 2018. Transcriptome comparison of meniscus
459 from patients with and without osteoarthritis. Osteoarthritis Cartilage 26:422-432.
460 41. Muhammad H, Schminke B, Bode C, et al. 2014. Human migratory meniscus
461 progenitor cells are controlled via the TGF-β pathway. Stem Cell Reports 3:789-
462 803.
463 42. Sun H, Wen X, Li H, et al. 2020. Single-cell RNA-seq analysis identifies meniscus
464 progenitors and reveals the progression of meniscus degeneration. Ann Rheum
465 Dis 79:408-417.
466 43. Rovinski D, Ramos RB, Fighera TM, et al. 2018. Risk of venous thromboembolism
467 events in postmenopausal women using oral versus non-oral hormone therapy: A
468 systematic review and meta-analysis. Thromb Res 168:83-95.
469 44. Beral V. 2003. Breast cancer and hormone-replacement therapy in the Million
470 Women Study. Lancet 362:419-427.
471 45. Taylor HS, Manson JE. 2011. Update in hormone therapy use in menopause. J
472 Clin Endocrinol Metab 96:255-264.
473 46. Rothrauff BB, Yang G, Tuan RS. 2017. Tissue-specific bioactivity of soluble
474 tendon-derived and cartilage-derived extracellular matrices on adult mesenchymal
475 stem cells. Stem Cell Res Ther 8:133.
476 47. Tarafder S, Gulko J, Kim D, et al. 2019. Effect of dose and release rate of CTGF
477 and TGFβ3 on avascular meniscus healing. J Orthop Res 37:1555-1562.
478 48. Yuan X, Wei Y, Villasante A, et al. 2017. Stem cell delivery in tissue-specific
479 hydrogel enabled meniscal repair in an orthotopic rat model. Biomaterials 132:59-
480 71.

481 49. Huey DJ, Athanasiou KA. 2011. Maturational growth of self-assembled, functional
482 menisci as a result of TGF-β1 and enzymatic chondroitinase-ABC stimulation.
483 Biomaterials 32:2052-2058.
484 50. MacBarb RF, Makris EA, Hu JC, et al. 2013. A chondroitinase-ABC and TGF-β1
485 treatment regimen for enhancing the mechanical properties of tissue-engineered
486 fibrocartilage. Acta Biomater 9:4626-4634.
487 51. Wang Q, Tan Q, Xu W, et al. 2018. Postnatal deletion of Alk5 gene in meniscal
488 cartilage accelerates age-dependent meniscal degeneration in mice. J Cell Physiol
489 234:595-605.
490 52. Valcourt U, Alcaraz LB, Exposito JY, et al. 2015. Tenascin-X: beyond the
491 architectural function. Cell Adh Migr 9:154-165.
492 53. Robertson IB, Horiguchi M, Zilberberg L, et al. 2015. Latent TGF-β-binding
493 proteins. Matrix Biol 47:44-53.
494 54. Fragiadaki M, Ikeda T, Witherden A, et al. 2011. High doses of TGF-β potently
495 suppress type I collagen via the transcription factor CUX1. Mol Biol Cell 22:1836-
496 1844.
497 55. Son MS, Levenston ME. 2017. Quantitative tracking of passage and 3D culture
498 effects on chondrocyte and fibrochondrocyte gene expression. J Tissue Eng
499 Regen Med 11:1185-1194.
500 56. Jones JC, Burks R, Owens BD, et al. 2012. Incidence and risk factors associated
501 with meniscal injuries among active-duty US military service members. J Athl Train
502 47:67-73.
503
504

505 **Figure Legends**

506 **Figure 1:** Experimental design. Cells were isolated from the medial meniscus of two 47-year old
507 donors, one of each sex, and treated with two concentrations of E2 under pulsed and continuous
508 conditions. RNA-Seq was then used to analyze the samples. Running silhouettes from freepik.com.

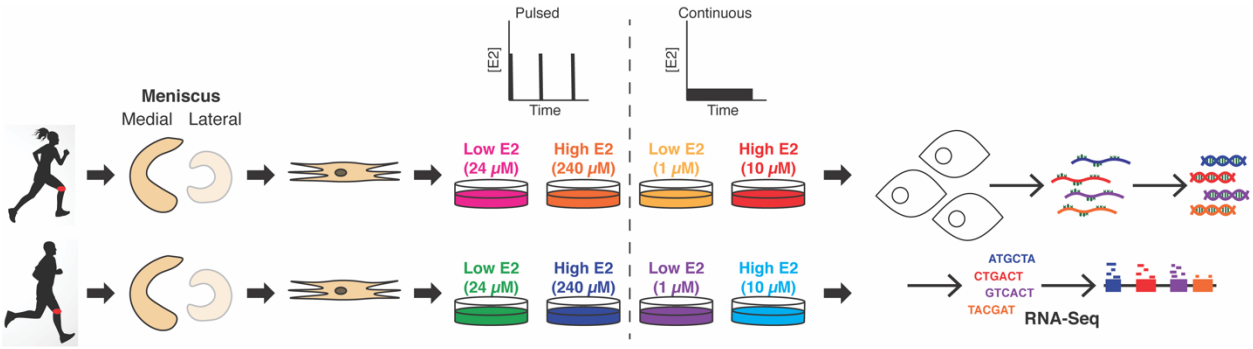

509

510

511 **Figure 2:** Visualization of the number of differentially expressed genes (DEGs) by treatment
512 group in comparison to physiological serum estrogen concentrations.

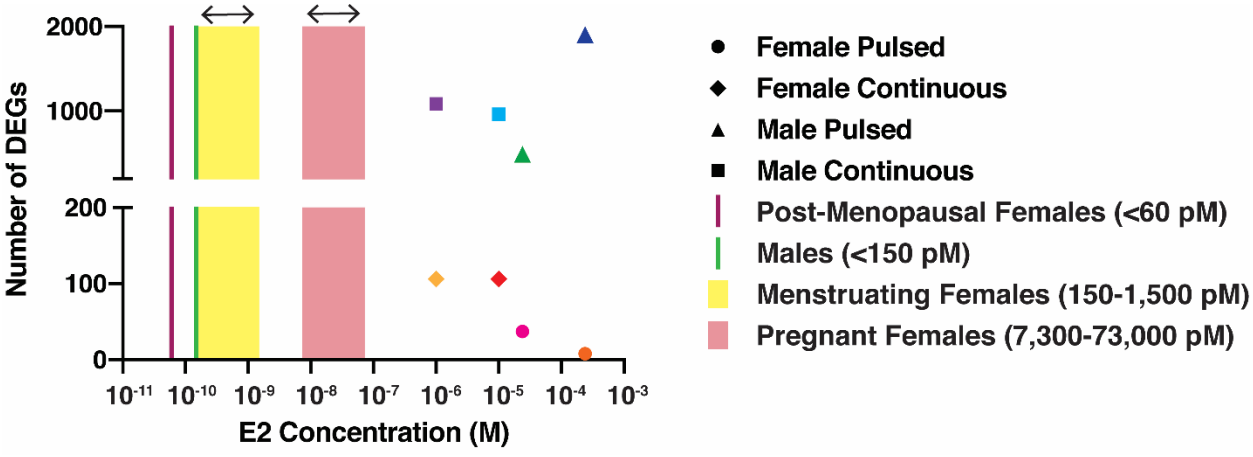

513

514

515 **Figure 3:** Visualization of differentially expressed genes (DEGs). Volcano plots and Venn
516 diagrams (Venny 2.1) illustrate the number of differentially expressed genes in each treatment
517 group. Only DEGs with padj<0.05 were used in the Venn diagrams.

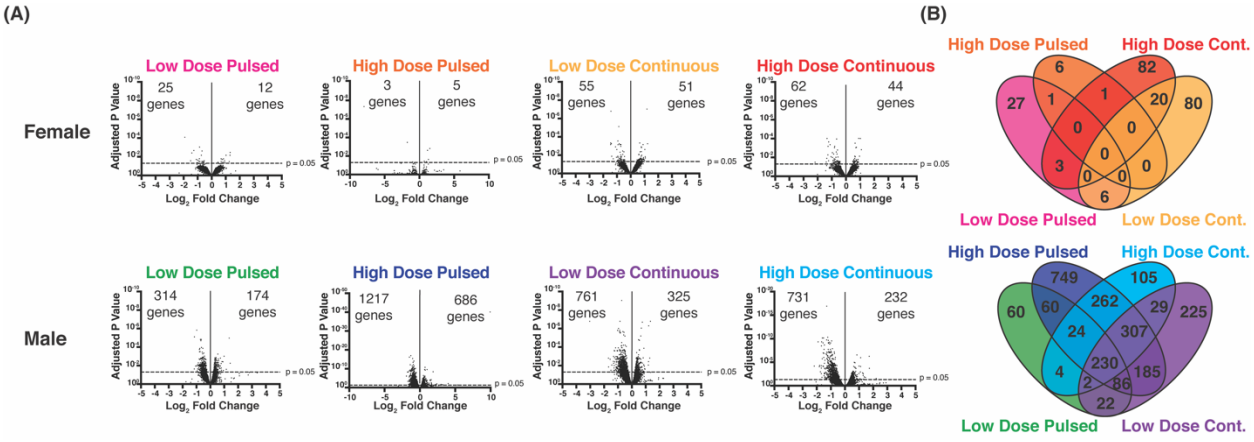

Figure 4: STRING analysis of DEGs from all 4 continuous dosing treatment groups. Images are shown as confidence views, where associations with stronger data support are thicker. Only DEGs with padj<0.05 are shown. Additional constraints based on log_2FoldChange were used to limit DEGs to a reasonable number for plotting and to highlight those with greater log_2FoldChanges. For the female groups, only log_2FoldChange >0.5 or <-0.5 are shown. For the male groups, only log_2FoldChange >1.0 or <-1.0 are shown. Color coding is based on functional enrichment analysis within STRING and is indicated for each treatment group. Abbreviations: GO-Gene Ontology, KEGG-Kyoto Encyclopedia of Genes and Genomes, ECM-extracellular matrix.

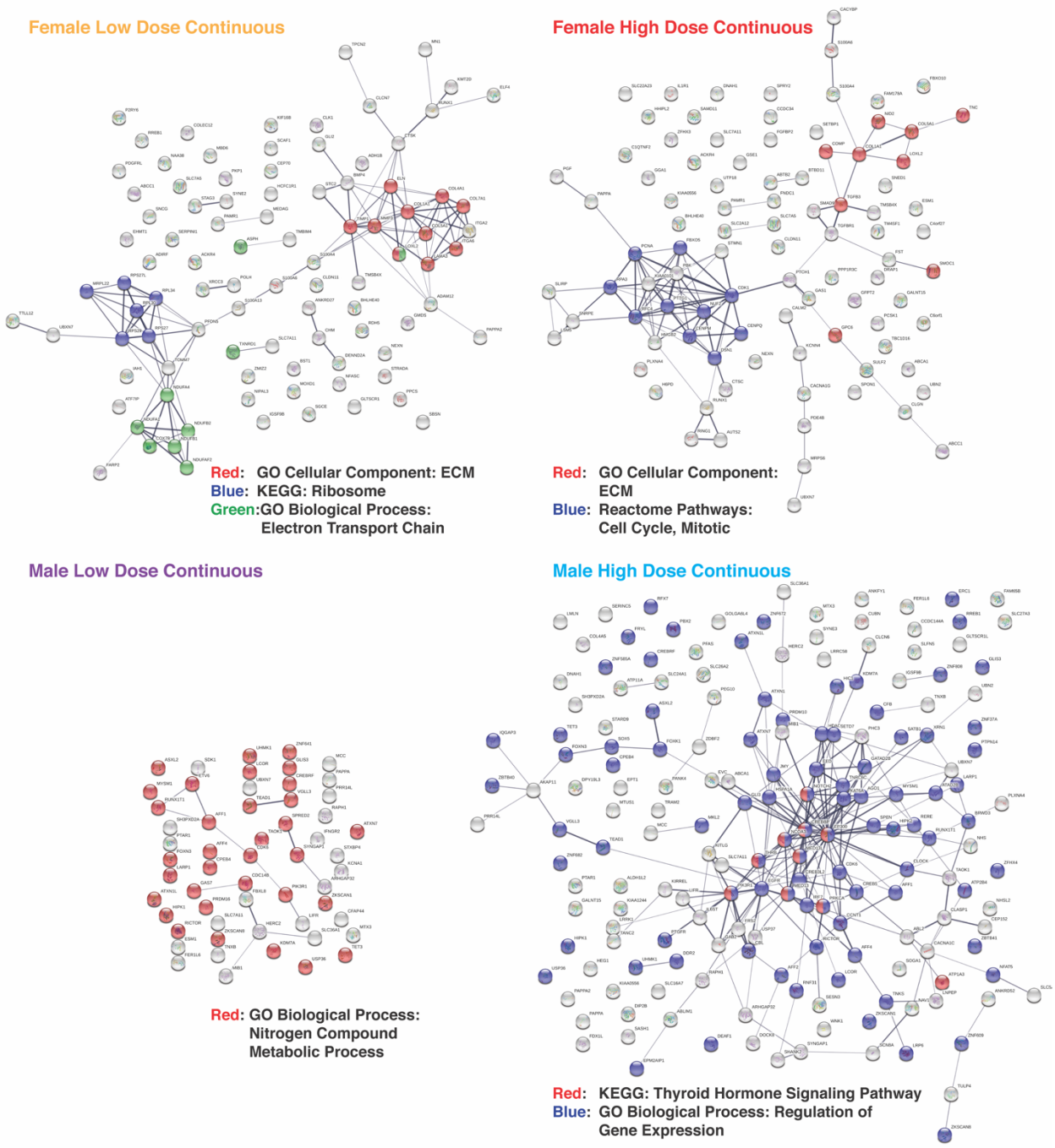

528

529

530 **Figure 5:** Analysis of the response of both sexes to the same treatment. (A) Venn diagrams (Venny

531 2.1) were generated to show which genes were altered in both sexes under the same treatment. For

532 treatments with more than one common gene, functional enrichment analysis was performed using

533 (B) DAVID and (C) STRING analysis to determine what types of genes were differentially
534 expressed. Functional enrichment analysis shows the Gene Ontology Cellular Component groups
535 with p values<0.05. STRING analysis shows known and predicted interactions between the
536 proteins encoded by the genes in confidence views, where associations with stronger data support
537 are thicker.

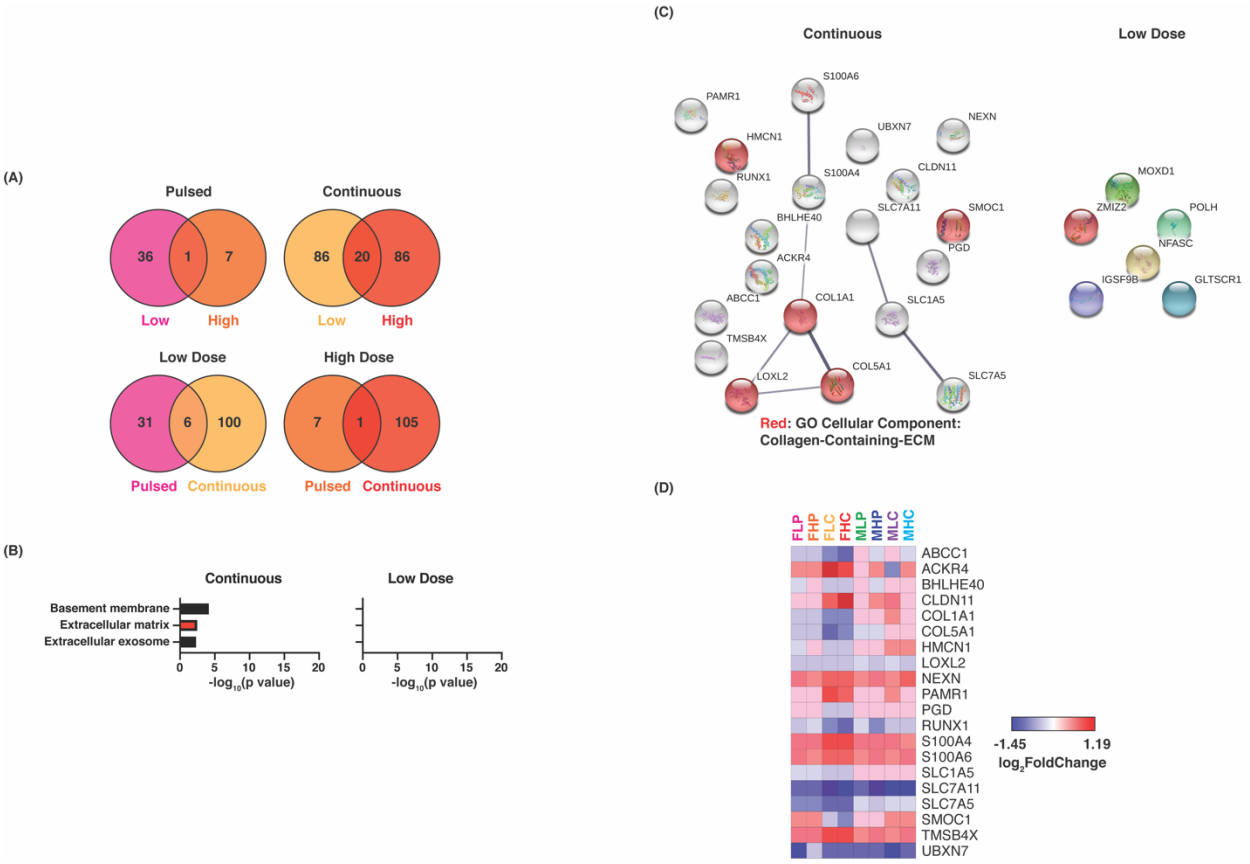

538

539

540 **Figure 6:** Analysis of DEGs that overlap between any two female treatment groups. (A) Venn
541 diagrams (Venny 2.1) were generated to show which genes were altered in more than one treatment
542 group. For groups with more than one common gene, functional enrichment analysis was
543 performed using (B) DAVID and (C) STRING analysis to determine what types of genes were
544 differentially expressed. (D) A heat map was generated of all 20 DEGs that were present in both

545 continuous treatment groups. Functional enrichment analysis shows the Gene Ontology Cellular
546 Component groups with p values<0.05. STRING analysis shows known and predicted interactions
547 between the proteins encoded by the genes in confidence views, where associations with stronger
548 data support are thicker. Heat map was generated using GenePattern. Genes are listed in
549 alphabetical order. Values shown are log_2FoldChange of each gene for each treatment group as
550 compared to the sex-matched no E2 control.

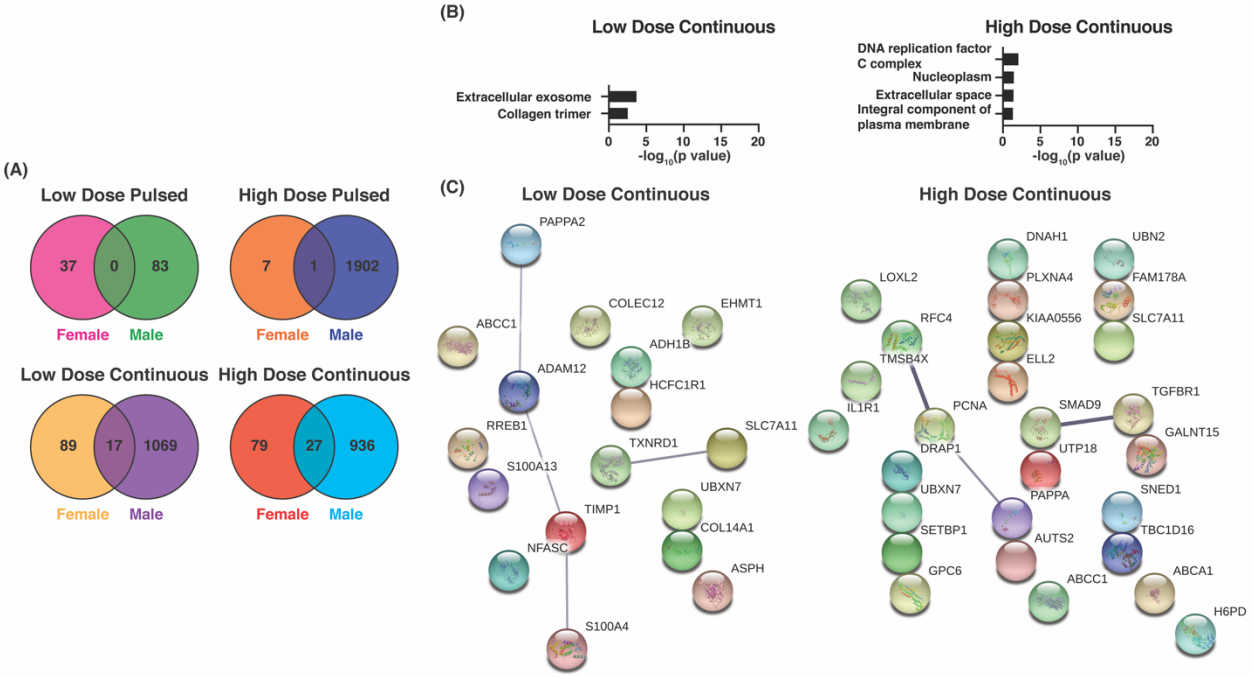

551

552

553 **Figure 7:** Functional enrichment analysis of DEGs using DAVID. Categories shown are from the
554 Gene Ontology Cellular Component database. Where available, the top 15 groups by p value are
555 shown with only p values < 0.05 considered.

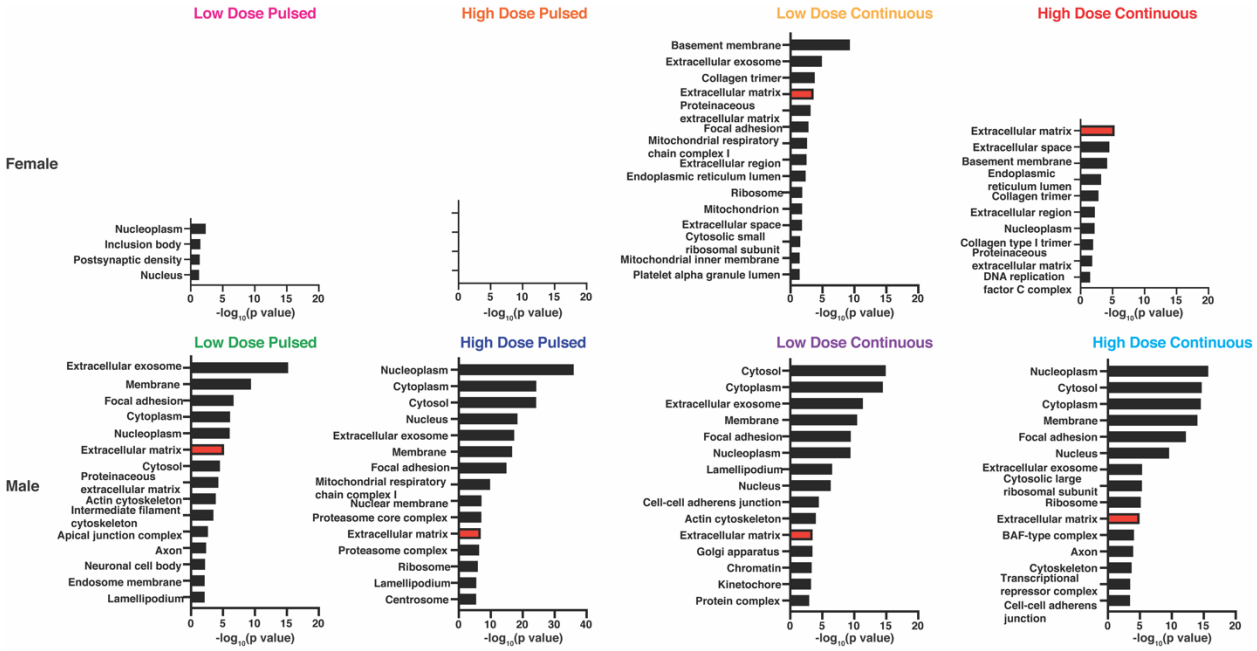

556

557

558 **Figure 8:** Heat map of extracellular matrix gene expression. Heat map was generated using

559 GenePattern. Genes are listed in alphabetical order. Values shown are $\log_2$FoldChange of each

560 gene for each treatment group as compared to the sex-matched no E2 control.

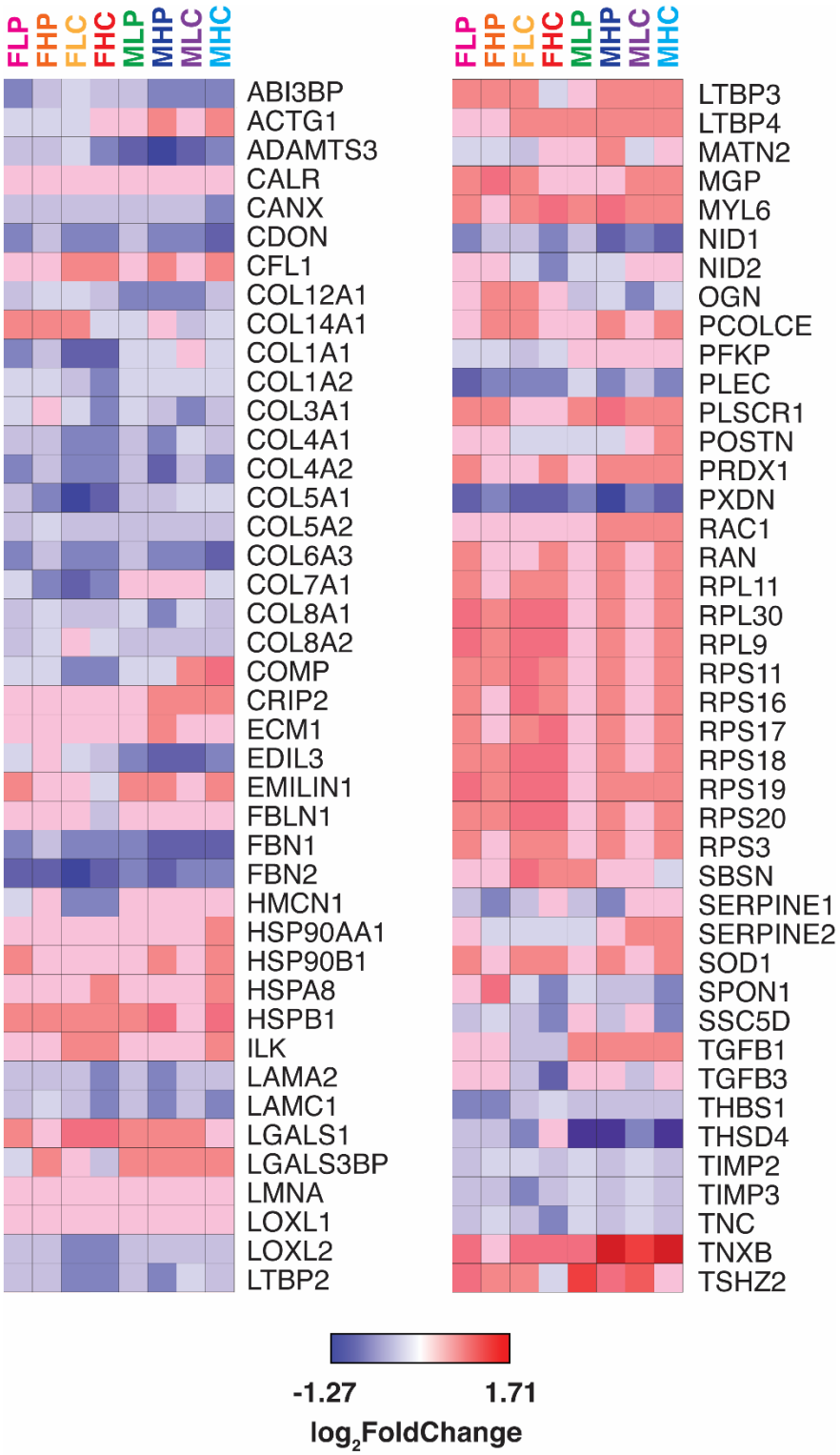
FLP
FHP
FLC
FHC
MLP
MHP
MLC
MHC
ABI3BP
ACTG1
ADAMTS3
CALR
CANX
CDON
CFL1
COL12A1
COL14A1
COL1A1
COL1A2
COL3A1
COL4A1
COL4A2
COL5A1
COL5A2
COL6A3
COL7A1
COL8A1
COL8A2
COMP
CRIP2
ECM1
EDIL3
EMILIN1
FBLN1
FBN1
FBN2
HMCN1
HSP90AA1
HSP90B1
HSPA8
HSPB1
ILK
LAMA2
LAMC1
LGALS1
LGALS3BP
LMNA
LOXL1
LOXL2
LTBP2
LTBP3
LTBP4
MATN2
MGP
MYL6
NID1
NID2
OGN
PCOLCE
PFKP
PLEC
PLSCR1
POSTN
PRDX1
PXDN
RAC1
RAN
RPL11
RPL30
RPL9
RPS11
RPS16
RPS17
RPS18
RPS19
RPS20
RPS3
SBSN
SERPINE1
SERPINE2
SOD1
SPON1
SSC5D
TGFB1
TGFB3
THBS1
THSD4
TIMP2
TIMP3
TNC
TNXB
TSHZ2
-1.27
1.71
log2FoldChange

561